





Cite this: *Chem. Sci.*, 2021, 12, 10306

All publication charges for this article have been paid for by the Royal Society of Chemistry

# Dynamic parallel kinetic resolution of $\alpha$ -ferrocenyl cation initiated by chiral Brønsted acid catalyst†

Yasunori Toda,  <sup>‡a</sup> Toshinobu Korenaga,  <sup>b</sup> Ren Obayashi,<sup>a</sup> Jun Kikuchi  <sup>a</sup> and Masahiro Terada  <sup>\*a</sup>

The dynamic parallel kinetic resolution (DPKR) of an  $\alpha$ -ferrocenyl cation intermediate under the influence of a chiral conjugate base of a chiral phosphoric acid catalyst has been demonstrated in an  $S_N1$  type substitution reaction of a racemic ferrocenyl derivative with a nitrogen nucleophile. The present method provides efficient access to a ferrocenylethylamine derivative in a highly enantioselective manner, which is potentially useful as a key precursor of chiral ligands for metal catalysis. The mechanism of the present intriguing resolution system was elucidated by control experiments using the enantio-pure precursor of relevant  $\alpha$ -ferrocenyl cation intermediates and the hydroamination of vinylferrocene. Further theoretical studies enabled the elucidation of the origin of the stereochemical outcome as well as the efficient DPKR. The present DPKR, which opens a new frontier for kinetic resolution, involves the racemization process through the formation of vinylferrocene and the chemo-divergent parallel kinetic resolution of the enantiomeric  $\alpha$ -ferrocenyl cations generated by the protonation/deprotonation sequence of vinylferrocene.

Received 15th April 2021  
Accepted 28th June 2021

DOI: 10.1039/d1sc02122b

rsc.li/chemical-science

## Introduction

The kinetic resolution (KR) of racemic mixtures is one of the most fundamental and powerful methods for the preparation of enantiomerically enriched compounds.<sup>1</sup> In general, KR occurs because the two enantiomers of a racemic substrate react at different rates. To date, electronically neutral substrates, namely, non-charged organic molecules, have been employed in KR reactions.<sup>1d,2</sup> On the other hand, cationic molecules, despite being attractive chemical species, have rarely been used as KR reactants<sup>3,4</sup> and thus the development of an efficient method for the resolution of racemic cations under catalytic conditions is expected to open a new frontier for KR. Cationic molecules are attractive because they are common reactive species and often invoked as key intermediates in typical Brønsted acid catalysis. In particular, during the past decades, chiral phosphoric acids (CPAs) have emerged as effective Brønsted acid catalysts for enantioselective electrophilic activation. In fact, CPAs have enabled a wide variety of enantioselective transformations<sup>5,6</sup> in which the chiral conjugate base of a CPA catalyst functions as

a powerful stereocontrolling element.<sup>7</sup> Hence, it is naturally expected that the catalytic KR of a racemic cationic species using the chiral conjugate base of CPA would expand the scope of KR.<sup>8</sup> The method would not only establish a novel class of fundamental strategies for asymmetric synthesis, but also empower chiral Brønsted acid catalysis as the master of cation control.

The challenge of governing the reactivity of racemic cationic molecules as active intermediates using a chiral conjugate base has inspired the design of a fascinating resolution system. A CPA-catalysed  $S_N1$  type substitution reaction of  $\alpha$ -ferrocenyl alcohol derivatives is a viable and attractive approach to accomplish the KR of a racemic cationic molecule. In principle, the substitution at the  $\alpha$ -position of ferrocenyl alcohol derivatives should proceed through a stepwise pathway (Fig. 1).<sup>9</sup> Elimination occurs as the initial step, generating an  $\alpha$ -ferrocenyl cation,<sup>10</sup> and subsequent addition of a nucleophile to the cation affords a substitution product. More importantly, the chirality at the  $\alpha$ -position is completely preserved in a retentive manner during the course of the reaction because the central chirality at the  $\alpha$ -position of ferrocenyl derivatives is cleanly transformed into the “planar” chirality of the cation *via* neighbouring group participation of the iron centre. It should be pointed out that the chiral cation does not undergo racemization in this particular type of substitution reaction. Taking into consideration the unique features of this cationic intermediate, we envisioned that cation **A** generated from racemic ferrocenyl derivative **1** using CPA catalyst **2** would be resolved in the reaction with nitrogen nucleophile **3** (Fig. 2).<sup>11,12</sup> In the present

<sup>a</sup>Department of Chemistry, Graduate School of Science, Tohoku University, Aoba-ku, Sendai 980-8578, Japan. E-mail: mterada@tohoku.ac.jp; ytoda@shinshu-u.ac.jp; Web: <http://www.orgreact.sakura.ne.jp/en-index.html>

<sup>b</sup>Department of Chemistry and Biological Sciences, Faculty of Science and Engineering, Iwate University, Morioka 020-8551, Japan

† Electronic supplementary information (ESI) available: Experimental procedures and spectroscopic data for all new compounds. See DOI: 10.1039/d1sc02122b

‡ Present address: Department of Materials Chemistry, Faculty of Engineering, Shinshu University, Nagano 380-8553, Japan.

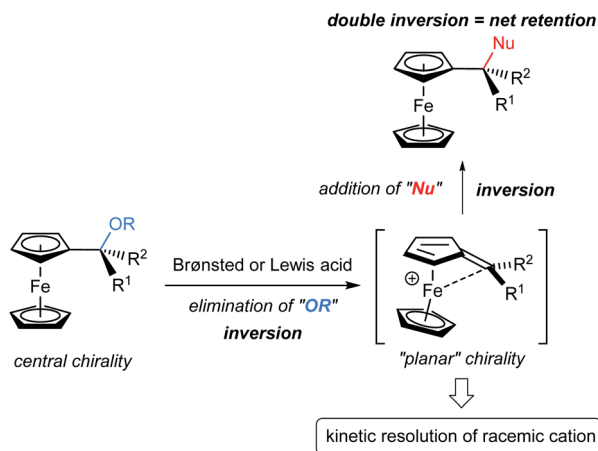


Fig. 1 Stereoretentive substitution at  $\alpha$ -position of ferrocenyl derivatives and application of cationic intermediate to KR.

characteristic KR, the competition between the substitution and elimination reactions would take place in parallel during the resolution. We thus assumed that both the substitution product, ferrocenylethylamine derivative **4**, and the elimination product, vinylferrocene (**5**), would be ideally formed in a comparable fashion and hence the chemo-divergent parallel kinetic resolution (PKR)<sup>13</sup> of  $\alpha$ -ferrocenyl cation **A** would be feasible. Because only a limited number of PKRs have been reported, it is of particular interest whether the use of racemic cation **A** enables the present unique PKR under the influence of the chiral conjugate base of CPA **2**. In addition, vinylferrocene (**5**) can be readily converted into racemic methyl ether **1** through the addition of methanol to the vinyl moiety of **5** in the presence of a strong Brønsted acid,<sup>§</sup> and regenerated **1** is subjected to the same reaction sequence. Therefore, a formal dynamic kinetic resolution (DKR)<sup>14</sup> would be established by the present method.

Keeping the above postulate in mind, we performed the  $S_N1$  type substitution reaction of racemic ferrocenyl derivative **1** with nitrogen nucleophile **3** catalysed by CPA **2** ( $G = 9$ -anthryl).

Herein we disclose the formation of highly enantio-enriched ferrocenylethylamine derivative **4**, which has been potentially useful as a key precursor of chiral ligands for metal catalysis,<sup>9,15</sup> by virtue of the distinctive KR of racemic  $\alpha$ -ferrocenyl cation **A**. In the present resolution system, it was confirmed that DKR, namely, the involvement of a racemization process between enantiomeric cations **A**, also occurs simultaneously during PKR of these cations. Mechanistic studies revealed that the formation of vinylferrocene (**5**) and its protonation/deprotonation sequence are the key to accomplishing the present intriguing resolution system, termed "dynamic PKR (DPKR)".

## Results and discussion

The initial experiment was performed using racemic **1**, 5 mol% of CPA ( $R$ )-**2** ( $G = 9$ -anthryl), 0.5 equivalent of 4-toluenesulfonamide (**3a**), and molecular sieve (MS) 5A in toluene at room temperature for 6 h (Table 1, entry 1). The reaction cleanly afforded substitution product **4** with moderate enantioselectivity and elimination product **5**. Then, screening for catalysts, solvents, and temperatures was conducted; however, none of the conditions led to an improvement in the initial result (see ESI† for details). Importantly, investigation of amine nucleophiles **3** revealed that the  $N$ -protecting group strongly affected both reactivity and enantioselectivity (Table 1, entries 1–7).<sup>11a</sup> Whereas relatively nucleophilic 4-anisidine (**3b**) and other nitrogen nucleophiles, such as phosphinamide **3c** and carbamate **3d**, exhibited poor reactivity (Table 1, entries 2–4), less nucleophilic **3f** and **3g** bearing electron-withdrawing 4- and 2-nitrobenzenesulfonyl groups, respectively, were crucial for achieving high enantioselectivity (Table 1, entries 6 and 7). In particular, the reaction of 2-nitrobenzenesulfonamide (nosylamide: **3g**) afforded substitution product ( $S$ )-**4g** in 95% ee (Table 1, entry 7), and the best chemo- and stereocontrol was achieved when 2.0 equivalents of nosylamide (**3g**) was employed (Table 1, entry 8).

The present reaction proceeds in a stepwise manner. First, the C–O bond cleavage by CPA ( $R$ )-**2** generates  $\alpha$ -ferrocenyl

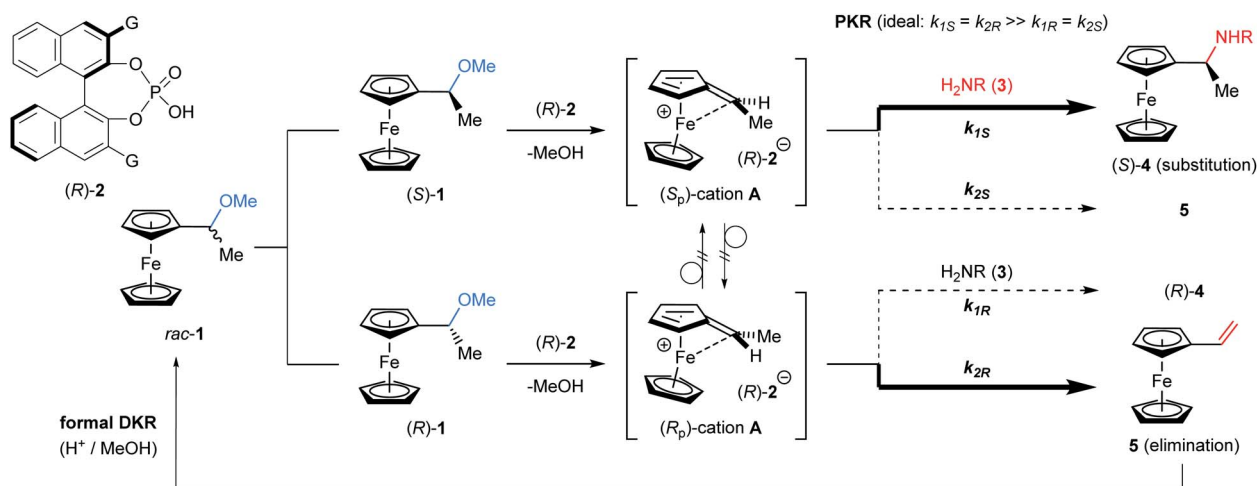
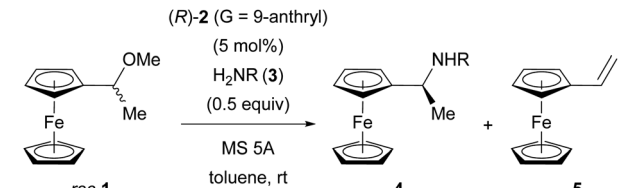


Fig. 2 Proposal: parallel kinetic resolution of  $\alpha$ -ferrocenyl cation catalysed by CPA.



**Table 1** Screening for amine nucleophiles in the parallel kinetic resolution of  $\alpha$ -ferrocenyl cation<sup>a</sup>


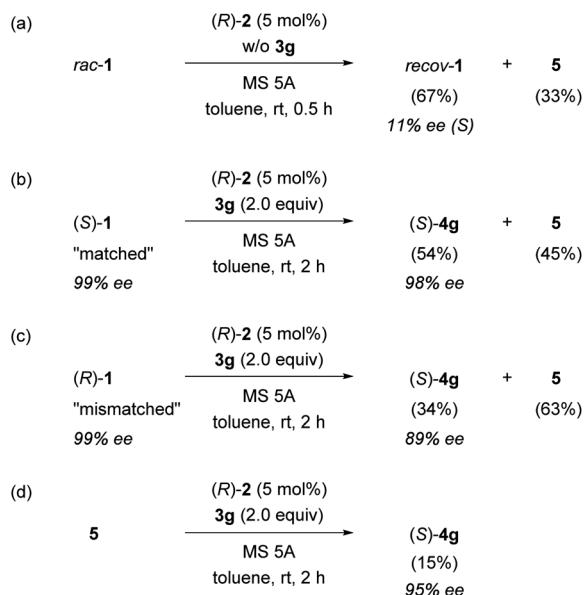
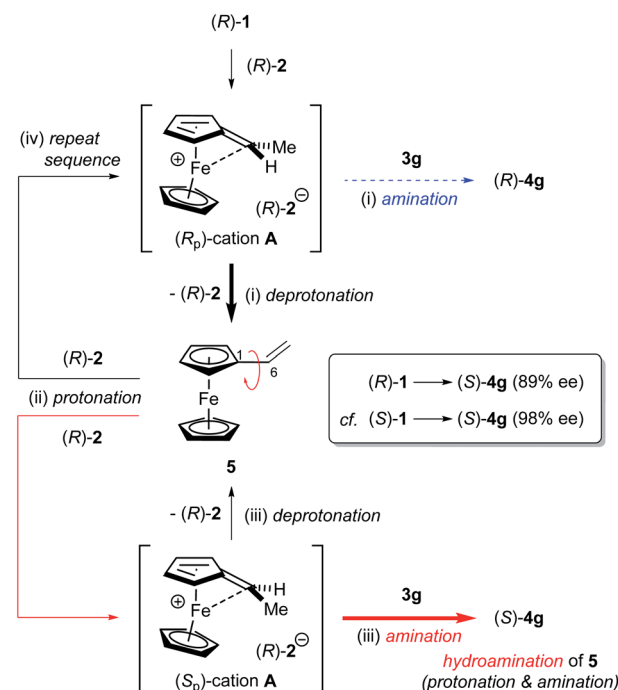
Entry	3: R	Time (h)	Yield <sup>b</sup> (%) 4/5	ee <sup>c</sup> (%)
1	3a: Ts	6	50/50	40
2	3b: 4-MeOC <sub>6</sub> H <sub>4</sub>	24	<5	—
3	3c: Ph <sub>2</sub> (O)P	24	<5	—
4	3d: Cbz	24	34/26	<1
5	3e: 4-MeOC <sub>6</sub> H <sub>4</sub> SO <sub>2</sub>	6	50/50	28
6	3f: 4-NO <sub>2</sub> C <sub>6</sub> H <sub>4</sub> SO <sub>2</sub>	2	44/52	82
7	3g: 2-NO <sub>2</sub> C <sub>6</sub> H <sub>4</sub> SO <sub>2</sub> (Ns)	2	40/60	95
8 <sup>d</sup>	3g	2	47(47)/51(43)	95

<sup>a</sup> Unless otherwise noted, all reactions were performed using 0.20 mmol of **1**, 5 mol% of catalyst **2**, and 0.5 equivalent of **3** in toluene (0.2 M) at room temperature. <sup>b</sup> Determined by crude <sup>1</sup>H NMR analysis (in C<sub>6</sub>D<sub>6</sub>) using 1,3-benzodioxole as the internal standard. Isolated yields are shown in parentheses. <sup>c</sup> Determined by chiral stationary phase HPLC analysis. <sup>d</sup> 2.0 equivalents of **3g** was used. The absolute configuration of **4g** was determined by derivatization into a known compound. See ESI for details.

cation **A**, and then the C–N bond formation (amination) by nosylamide (**3g**) yields substitution product (*S*)-**4g** or the deprotonation affords **5**. As shown in Table 1, the amine nucleophile had the greatest impact on the enantioselectivity with respect to both the substituent and the number of

equivalents, and it seems that the second step would be the key to achieving efficient KR. To confirm the proposed mechanism, a control experiment was performed in the reaction without using nucleophile **3g** and the reaction was quenched prior to complete conversion (Fig. 3a). As expected, the reaction in the absence of **3g** resulted in the recovery of nearly racemic **1**, clearly suggesting that there is only a slight difference in the reaction rate between enantiomers **1** in the C–O bond cleavage step. Again, it is worth noting that the influence of the nucleophile on the enantioselectivity is a further indication that the resolution occurs in the second step, in which competitive amination and deprotonation reactions take place.

Next, the mechanism was further investigated using enantiopure starting material **1**. Based on the efficiency of the observed KR, it was assumed that (*S<sub>p</sub>*)-cation **A** generated from (*S*)-**1** and chiral conjugate base (*R*)-**2**<sup>−</sup> would undergo C–N bond formation (amination) with **3g** to afford (*S*)-**4g** smoothly (C–N matched), whereas (*R*)-**1** would selectively lead to the formation of vinylferrocene (**5**) via (*R<sub>p</sub>*)-cation **A** (C–N mismatched). As expected, (*S*)-**1** (99% ee) gave (*S*)-**4g** (98% ee) with nearly complete retention of chirality. However, it is worth mentioning that the formation of a considerable amount of vinylferrocene (**5**) was also observed (Fig. 3b). In contrast, in the reaction of the mismatched combination, namely, enantiopure (*R*)-**1** and CPA (*R*)-**2**, elimination product **5** was formed as the major product (Fig. 3c). More interestingly, a small amount of (*S*)-**4g** was obtained with inversion at the stereogenic center (89% ee), despite the fact that the nucleophilic substitution of ferrocenyl alcohol derivatives generally proceeds in a retentive manner.


**Fig. 3** Mechanistic studies using (*R*)-**2** (G = 9-anthryl): (a) the kinetic resolution of racemic **1** in the absence of **3g**. (b) The substitution reaction of enantiopure (*S*)-**1** with **3g**. (c) The substitution reaction of enantiopure (*R*)-**1** with **3g**. (d) The hydroamination of **5** with **3g**.**Fig. 4** Proposed mechanism for the formation of anomalous inversion product (*S*)-**4g** from (*R*)-**1** and the racemization process between (*S<sub>p</sub>*)- and (*R<sub>p</sub>*)-cations **A** through vinylferrocene (**5**).

The formation of anomalous inversion product (*S*)-**4g** from (*R*)-**1** is presumably rationalized by the enantioselective hydroamination of **5** catalysed by CPA **2** after elimination of methanol from (*R*)-**1**, as shown in Fig. 4: (i) (*R<sub>p</sub>*)-cation **A** generated from (*R*)-**1** is resolved by chiral conjugate base (*R*)-**2**<sup>−</sup>, affording **5** as the major product along with a small amount of retentive substitution product (*R*)-**4g**; (ii) elimination product **5** is further protonated at the double bond by CPA **2** to generate enantiomeric (*S<sub>p</sub>*)- and (*R<sub>p</sub>*)-cations **A**; (iii) because of the matched combination of (*S<sub>p</sub>*)-cation **A** and (*R*)-**2**<sup>−</sup>, the nucleophilic attack of **3g** on (*S<sub>p</sub>*)-cation **A** gives rise to (*S*)-**4g** with inversion at the stereogenic centre from initial (*R*)-**1**, although the deprotonation also takes place, affording **5** to some extent, as shown in Fig. 3b; and (iv) (*R<sub>p</sub>*)-cation **A** repeats the same resolution process as proposed above.

To confirm whether the enantioselective hydroamination of **5** by CPA **2** is involved in the present reaction, **5** was treated with nosylamide (**3g**) under the optimized reaction conditions (Fig. 3d). As expected, hydroamination product (*S*)-**4g** was obtained with high enantioselectivity (95% ee) even though the reaction was considerably sluggish and thus resulted in a diminished yield of (*S*)-**4g**. The enantiomeric excess (ee) of **4g** [89% ee (*S*), Fig. 3c] obtained from (*R*)-**1** was lower than that [95% ee (*S*), Fig. 3d] in the hydroamination of **5** because a small amount of product (*R*)-**4g** was furnished *via* the retentive substitution reaction of (*R*)-**1**. The ee observed in Fig. 3c is the sum of the stereochemical outcomes obtained for this retentive substitution and the hydroamination of **5**. Hence, these results are consistent with the proposed mechanism.

As depicted in Fig. 4, the overall scheme for the enantioselective hydroamination of vinylferrocene (**5**) with **3g** under the influence of CPA catalyst (*R*)-**2** is also well described. It is pointed out that during the protonation/deprotonation sequence of **5**, the free rotation around the C<sub>1</sub>–C<sub>6</sub> single bond of **5** enables one enantiomer of **A** to isomerize into the other. Thus, the racemization between (*S<sub>p</sub>*)- and (*R<sub>p</sub>*)-cations **A** is allowed through the formation of vinylferrocene (**5**), although the direct racemization of enantiomeric cations **A** is absolutely prevented by the ferrocenyl neighboring effect. More importantly, the substitution of racemic **1** and the hydroamination of **5** exhibited the same enantioselectivity (95% ee) and hence it is considered that both the hydroamination and the substitution reaction proceed through common cation **A**.

In order to acquire insights into the origin of the stereochemical outcome and elucidate the present resolution system, we theoretically pursued the transition states in the C–N bond formation (amination) step, namely, the resolution step, of enantiomeric cations **A** with sulfonamide nucleophile **3g** under the influence of chiral conjugate base (*R*)-**2**<sup>−</sup>. Geometrical optimization of transition states **TSs** and **TSr** leading to a pair of enantiomers (*S*)- and (*R*)-**4g**, respectively, was thoroughly conducted by DFT calculations.<sup>16–19</sup> As shown in Fig. 5, in optimized transition structures **TSs** and **TSr**, chiral conjugate base (*R*)-**2**<sup>−</sup> interacts not only with the N–H proton of sulfonamide nucleophile **3g** but also with a couple of protons of the vinylferrocene unit through hydrogen bonds. Thus, **TSs** and **TSr** feature multi-coordinating hydrogen bonds, which are an

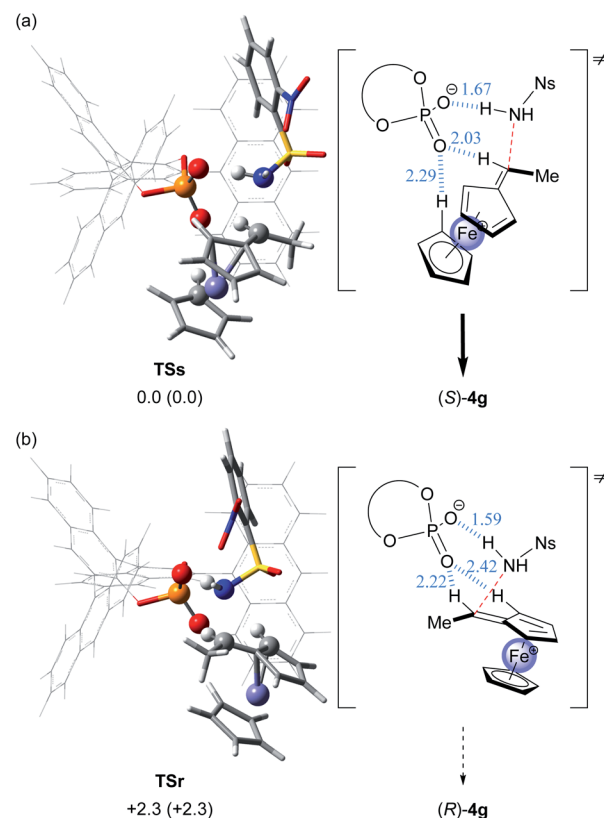


Fig. 5 3D structures and schematic representation models of the most energetically favorable transition states for the C–N bond formation step, **TSs** and **TSr**, are shown. The 3D structures of each fragment are represented as follows: ferrocene and nosylamide fragments and phosphoric acid subunit: “tube” model; iron and atoms involved in the hydrogen bonding interaction: “ball & bond type” model; and binaphthyl backbone and substituent (G): “wire” model. Relative free energies (kcal mol<sup>−1</sup>) obtained by single-point energy calculations are shown for the optimized transition states at the M06-2X/6-311+G\*\* level<sup>18</sup> in the solution phase according to the SCRf method based on CPCM<sup>19</sup> (toluene). Relative free energies (kcal mol<sup>−1</sup>) of the optimized structures at the B3LYP/6-31G\* level<sup>17</sup> in the gas phase are shown in parentheses. Hydrogen bond lengths are indicated in blue (angstroms): (a) (*S<sub>p</sub>*)-cation **A**/**3g**/*(R)*-**2**<sup>−</sup> (G = 9-anthryl) for **TSs**. (b) (*R<sub>p</sub>*)-cation **A**/**3g**/*(R)*-**2**<sup>−</sup> (G = 9-anthryl) for **TSr**.

essential interaction mode observed widely in CPA-catalysed reactions<sup>5–7</sup> and are beneficial for controlling the stereochemical outcome.<sup>20,21</sup> Among the interactions observed, it is noteworthy that the hydrogen bond is formed between the vinyl proton of cation **A** and the oxygen atom of chiral conjugate base (*R*)-**2**<sup>−</sup> in both transition states **TSs** and **TSr**.

The relative energy difference between **TSs** and **TSr** is sufficient for good stereochemical outcome in favor of **TSs** ( $\Delta\Delta G^\ddagger = 2.3$  kcal mol<sup>−1</sup>) and consistent with the experimental observation, namely, the formation of (*S*)-**4g** as the major product. However, in the present characteristic KR, the C–N bond formation (amination) and the deprotonation compete with each other in both reactions using enantiomeric substrates **1**, as shown in the control experiments (Fig. 3b and c). In the matched combination of (*S<sub>p</sub>*)-cation **A**/*(R)*-**2**<sup>−</sup>, these reactions are comparable and thus the transition state of the





deprotonation step and **TSs** are energetically similar. In contrast, the mismatched combination of (*R<sub>p</sub>*)-cation **A**/(*R*)-2<sup>−</sup> markedly facilitates the deprotonation and thus **TSr** is energetically unfavourable relative to the transition state of the deprotonation step. From the above considerations, it was assumed that in the deprotonation of enantiomeric cations **A** by chiral conjugate base (*R*)-2<sup>−</sup>, the energy difference between (*S<sub>p</sub>*)- and (*R<sub>p</sub>*)-cations **A** would not be significant. In fact, DFT calculations of the transition states revealed that the deprotonation of (*S<sub>p</sub>*)-cation **A** by chiral conjugate base (*R*)-2<sup>−</sup> is energetically comparable to that of (*R<sub>p</sub>*)-cation **A** ( $\Delta\Delta G^\ddagger = 0.3 \text{ kcal mol}^{-1}$ ).<sup>||</sup> More importantly, the backward reaction, namely, the protonation of vinylferrocene (**5**) by CPA (*R*)-2, also proceeds through the same transition states because of the equilibrium between cation **A** and **5**. Hence, the protonation of **5** by CPA (*R*)-2 affords a nearly racemic mixture of cation **A**.

As shown in Fig. 3d, the control experiment revealed that the protonation of vinylferrocene (**5**) by CPA (*R*)-2 occurred albeit in low efficiency. Furthermore, in the protonation of **5** by CPA (*R*)-2, the formation of a nearly racemic mixture of cation **A** is predicted by DFT studies. However, the efficient PKR of racemic cation **A** has been established in the substitution reaction of racemic **1** with **3g** as well as the hydroamination of **5** with **3g**, both of which proceed through the same cation **A**. More importantly, the racemization between (*S<sub>p</sub>*)- and (*R<sub>p</sub>*)-cations **A** is allowed through the formation of vinylferrocene (**5**). Integrating these features enabled us to establish the innovative system termed DPKR because the racemization process takes place prior to the resolution step. In order to achieve the intended DPKR of enantiomeric cations **A**, we further explored the reaction conditions to accelerate the protonation of **5** by CPA (*R*)-2 and also the formation of product **4g** efficiently. As shown in Fig. 6a, the use of chlorobenzene, instead of toluene, as the solvent facilitated the hydroamination of **5** with **3g** under the influence of CPA (*R*)-2 presumably because of the stabilization of cations **A** generated in the slightly polar solvent, chlorobenzene.<sup>\*\*</sup> The modification of the conditions resulted in the complete consumption

of **5**, affording (*S*)-**4g** in high yield without any detrimental effect on the enantioselectivity.

The amended method is also applicable to the substitution reaction of racemic **1** with **3g**, affording (*S*)-**4g** in comparable yield to the hydroamination while maintaining the high enantioselectivity (Fig. 6b vs. 6a). The established DPKR realized the enantio-convergent process in which both enantiomers of racemic **1** were transformed into single enantiomer (*S*)-**4g** in a nearly quantitative manner.<sup>22††</sup> In addition, the nosyl (Ns) group attached to the nitrogen atom of substitution product **4g** can be readily removed to afford the primary amine derivative (see ESI† for details), which has been widely used as an important precursor of chiral ligands for metal catalysis.<sup>9,15</sup> It should be emphasized again that the formation of vinylferrocene (**5**) is the key to allowing the racemization of enantiomeric cations **A** generated from racemic **1** or the protonation of **5**. Otherwise, it is impossible to achieve the present enantio-convergent process.

## Conclusions

We have demonstrated the dynamic parallel kinetic resolution (DPKR) of an  $\alpha$ -ferrocenyl cation under the influence of a chiral conjugate base of a phosphoric acid catalyst. The mechanism of the present intriguing resolution system was elucidated by control experiments using the enantio-pure precursor of the relevant  $\alpha$ -ferrocenyl cation intermediates and the hydroamination of vinylferrocene. Further theoretical studies enabled us to understand the origin of the stereochemical outcome as well as to establish an efficient DPKR. The present resolution system was accomplished by virtue of the dynamic racemization process of enantiomeric  $\alpha$ -ferrocenyl cations through vinylferrocene and the chemo-divergent PKR of these cations. The present method enables the formation of a ferrocenylethylamine derivative, which is a key precursor of chiral ligands for metal catalysis, in a nearly quantitative manner with high enantioselectivity. The established DPKR features the integrated aspects of conventional KR and related variants. Further development of an efficient and distinctive kinetic resolution system using chiral phosphoric acid and its derivatives is in progress.

## Data availability

The exploratory investigation, experimental procedures, computational data, and characterization data are available.

## Author contributions

Y. T.: conceptualization, data curation, formal analysis, investigation (experimental studies), and writing – original draft. T. K.: data curation, formal analysis, and investigation (theoretical studies). R. O.: data curation, formal analysis, and investigation (experimental studies). J. K.: data curation, formal analysis, and investigation (experimental studies). M. T.: conceptualization, project administration, writing – review & editing, supervision, and funding acquisition.

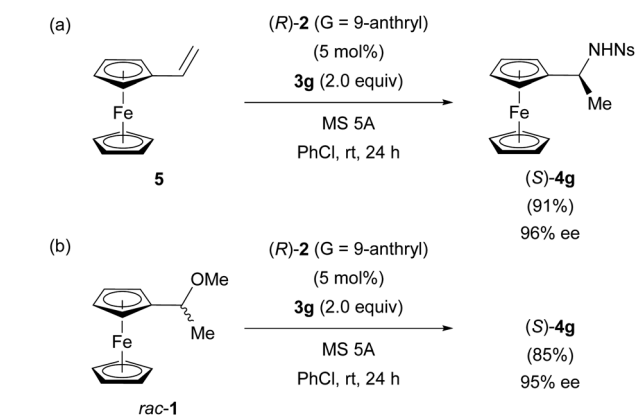


Fig. 6 DPKR of enantiomeric cations **A** using (*R*)-2 (G = 9-anthryl): (a) the hydroamination of **5** with **3g**. (b) The substitution reaction of racemic **1** with **3g** achieving enantio-convergent process.



## Conflicts of interest

There are no conflicts to declare.

## Acknowledgements

This work was partially supported by a Grant-in-Aid for Scientific Research on Innovative Areas “Advanced Molecular Transformations by Organocatalysts” (No. 23105002 & 26105704) and “Hybrid Catalysis for Enabling Molecular Synthesis on Demand” (No. JP17H06447) from MEXT, Japan. We also thank the Japan Society for the Promotion of Sciences for the JSPS Research Fellowship for Young Scientists (Y. T.).

## Notes and references

§ The acid-catalysed methanol addition to vinylferrocene (**5**) successfully regenerated methyl ether **1** in over 90% yield. See ESI† for details.

¶ All calculations were performed with the Gaussian 09 package.<sup>16</sup> Geometrical optimization of transition states **TSs** and **TSr** was conducted at the B3LYP/6-31G\* level<sup>17</sup> and characterized using frequency calculations, and the free energies were computed for the gas phase. Single-point energy calculations for the optimized transition states (at the B3LYP/6-31G\* level) were also evaluated at the M06-2X/6-311+G\*\* level<sup>18</sup> in the solution phase according to the SCRF method based on CPCM ( $\epsilon = 2.3741$  for toluene).<sup>19</sup> The free energies in toluene were calculated from the sum of the single-point energies in toluene and the value of thermal correction to Gibbs free energy in the gas phase.

|| All calculations were performed with the Gaussian 09 package.<sup>16</sup> The transition states of the deprotonation step of enantiomeric cations **A** by chiral conjugate base (*R*)-**2**<sup>−</sup> were optimized at the B3LYP/6-31G\* level<sup>17</sup> in the gas phase and characterized using frequency calculations. Single-point energy calculations for the optimized transition states were conducted at the M06-2X/6-311+G\*\* level<sup>18</sup> in the solution phase according to the SCRF method based on CPCM ( $\epsilon = 2.3741$  for toluene).<sup>19</sup> The free energies in toluene were calculated from the sum of the single-point energies in toluene and the value of thermal correction to Gibbs free energy in the gas phase.

\*\* The reaction in toluene under the same reaction conditions (at room temperature for 24 h) afforded (*S*)-**4g** in 24% yield with 94% ee.

†† In order to enhance the utility of the developed DPKR, we attempted the reaction of ferrocenyl derivative methyl ether having ethyl substituent, instead of methyl substituent of **1**. Initially, the optimized reaction conditions were applied to this derivative. However, demethoxylation product, namely, 1-propenylferrocene, was formed as the sole product and no desired substitution product was obtained at all, despite the complete consumption of the starting methyl ether. Similarly, the use of more nucleophilic TsNH<sub>2</sub> (**3a**) rather than NsNH<sub>2</sub> (**3g**) was also unsuccessful, affording 1-propenylferrocene quantitatively. These results indicate that protonation to 1-propenylferrocene became markedly sluggish using parent CPA (*R*)-**2**. Therefore CPAs having strong acidity, such as a triflylamide derivative and a bisphosphoric acid, were further investigated. As expected, these strong acids gave rise to the corresponding substitution product in moderate yield, albeit low enantioselectivity. The present intriguing DPKR is established by the well-balanced system between the deprotonation of cation **A** and the selective introduction of a nucleophile to enantiomeric cations **A**. Hence, to achieve the efficient DPKR with high enantioselectivity, optimization of CPAs and reaction conditions would be strictly required for each substrate. See ESI† for details.

- (a) H. B. Kagan and J. C. Fiaud, in *Topics in Stereochemistry*, ed. E. L. Eliel, Wiley & Sons, New York, 1988, vol. 18, pp. 249–330; (b) A. H. Hoveyda and M. T. Didiuk, *Curr. Org. Chem.*, 1998, **2**, 489–526; (c) J. M. Kieth, J. F. Larow and E. N. Jacobsen, *Adv. Synth. Catal.*, 2001, **1**, 5–26; (d) E. Vedejs and M. Jure, *Angew. Chem., Int. Ed.*, 2005, **44**, 3974–4001; (e) H. Pellissier, in *Separation of Enantiomers:*

*Synthetic Methods*, ed. M. H. Todd, Wiley & Sons, New York, 2014, pp. 75–89.

- Dynamic thermodynamic resolution has been reported by Beak *et al.*, see: (a) P. Beak, D. R. Anderson, M. D. Curtis, J. M. Laumer, D. J. Pippel and G. A. Weisenburger, *Acc. Chem. Res.*, 2000, **33**, 715–727; (b) W. K. Lee, Y. S. Park and P. Beak, *Acc. Chem. Res.*, 2009, **42**, 224–234.
- Some catalytic asymmetric reactions may proceed *via* the KR pathway for cationic intermediates under equilibrium conditions between the cations and the achiral reactants. In most of those cases, it is considered that enantio-enriched cationic intermediates are formed from the achiral reactants under the influence of chiral catalysts. See: (a) S. E. Denmark, W. E. Kuester and M. T. Burk, *Angew. Chem., Int. Ed.*, 2012, **51**, 10938–10953; (b) K. Murai and H. Fujioka, *Heterocycles*, 2013, **87**, 763–805.
- Jacobsen *et al.* reported the dynamic kinetic resolution of seleniranium ions, see: H. Zhang, S. Lin and E. N. Jacobsen, *J. Am. Chem. Soc.*, 2014, **136**, 16485–16488.
- For seminal studies, see: (a) T. Akiyama, J. Itoh, K. Yokota and K. Fuchibe, *Angew. Chem., Int. Ed.*, 2004, **43**, 1566–1568; (b) D. Uraguchi and M. Terada, *J. Am. Chem. Soc.*, 2004, **126**, 5356–5357.
- For selected reviews of chiral Brønsted acid catalysis, see: (a) H. Yamamoto and N. Payette, in *Hydrogen Bonding in Organic Synthesis*, ed. P. M. Pihko, Wiley-VCH, Weinheim, 2009, pp. 73–140; (b) T. Akiyama, *Chem. Rev.*, 2007, **107**, 5744–5758; (c) M. Terada, *Synthesis*, 2010, 1929–1982; (d) D. Kampen, C. M. Reisinger and B. List, *Top. Curr. Chem.*, 2010, **291**, 395–456; (e) D. Parmar, E. Sugiono, S. Raja and M. Rueping, *Chem. Rev.*, 2014, **114**, 9047–9153.
- For selected reviews of chiral anions in asymmetric catalysis, see: (a) R. J. Phipps, G. L. Hamilton and F. D. Toste, *Nat. Chem.*, 2012, **4**, 603–614; (b) M. Mahlau and B. List, *Angew. Chem., Int. Ed.*, 2013, **52**, 518–533; (c) K. Brak and E. N. Jacobsen, *Angew. Chem., Int. Ed.*, 2013, **52**, 534–561.
- For the enantio-convergent Nicholas reaction catalysed by chiral phosphoric acids, see: (a) M. Terada, Y. Ota, F. Li, Y. Toda and A. Kondoh, *J. Am. Chem. Soc.*, 2016, **138**, 11038–11043; (b) Y. Ota, A. Kondoh and M. Terada, *Angew. Chem., Int. Ed.*, 2018, **57**, 13917–13921.
- (a) T. Hayashi, in *Ferrocenes*, ed. A. Togni and T. Hayashi, VCH, Weinheim, Germany, 1995, pp. 105–142; (b) A. Togni, in *Metallocenes*, ed. A. Togni and R. L. Halterman, Wiley-VCH, Weinheim, Germany, 1998, vol. 2, pp. 685–721. See also: (c) A. Togni, C. Breutel, A. Schnyder, F. Spindler, H. Landert and A. Tajjani, *J. Am. Chem. Soc.*, 1994, **116**, 4062–4066; (d) P. Vicennati and P. G. Cozzi, *Eur. J. Org. Chem.*, 2007, 2248–2253.
- (a) A. A. Koridze, P. V. Petrovskii, S. P. Gubin, V. I. Sokolov and A. I. Mokhov, *J. Organomet. Chem.*, 1977, **136**, 65–71; (b) C. Bleiholder, F. Rominger and R. Gleiter, *Organometallics*, 2009, **28**, 1014–1017.
- For the enantioselective substitution reaction with nitrogen nucleophile using chiral phosphoric acids, see: (a) M. Rueping, U. Uriä, M.-Y. Lin and I. Atodiresei, *J. Am. Chem. Soc.*, 2011, **133**, 3732–3735; (b) P.-S. Wang,



- X.-L. Zhou and L.-Z. Gong, *Org. Lett.*, 2014, **16**, 976–979; (c) M. Zhuang and H. Du, *Org. Biomol. Chem.*, 2014, **12**, 4590–4593; (d) Y. Kuroda, S. Harada, A. Oonishi, Y. Yamaoka, K. Yamada and K. Takasu, *Angew. Chem., Int. Ed.*, 2015, **54**, 8263–8266; (e) J. Zhou and H. Xie, *Org. Biomol. Chem.*, 2018, **16**, 380–383; (f) M. Shimizu, J. Kikuchi, A. Kondoh and M. Terada, *Chem. Sci.*, 2018, **9**, 5747–5757.
- 12 T. Izumi and S. Aratani, *J. Chem. Technol. Biotechnol.*, 1995, **63**, 25–32.
- 13 (a) J. Eames, *Angew. Chem., Int. Ed.*, 2002, **39**, 885–888; (b) J. R. Dehli and V. Gotor, *Chem. Soc. Rev.*, 2002, **31**, 365–370.
- 14 For selected reviews of (dynamic) kinetic resolution, see: (a) K. S. Petersen, *Asian J. Org. Chem.*, 2016, **5**, 308–320; (b) R. Gurubrahmam, Y.-S. Cheng, W.-Y. Huang and K. Chen, *ChemCatChem*, 2016, **8**, 86–96; (c) V. Bhat, E. R. Welin, X. Guo and B. M. Stoltz, *Chem. Rev.*, 2017, **117**, 4528–4561.
- 15 (a) R. G. Arrayás, J. Adrio and J. C. Carretero, *Angew. Chem., Int. Ed.*, 2006, **45**, 7674–7715; (b) D. Schaarschmidt and H. Lang, *Organometallics*, 2013, **32**, 5668–5704.
- 16 M. J. Frisch, *et al.*, *Gaussian 09, Revision C.01*, Gaussian, Inc., Wallingford, CT, 2010, see ESI† for the full list of the authors.
- 17 (a) A. D. Becke, *Phys. Rev. A*, 1988, **38**, 3098–3100; (b) C. Lee, W. T. Yang and R. G. Parr, *Phys. Rev. B: Condens. Matter Mater. Phys.*, 1988, **37**, 785–789.
- 18 For M06-2X, see: Y. Zhao and D. G. Truhlar, *Theor. Chem. Acc.*, 2008, **120**, 215–241.
- 19 For CPCM, see: V. Barone and M. Cossi, *J. Phys. Chem. A*, 1998, **102**, 1995–2001.
- 20 For a review of computational studies of chiral Brønsted acid catalysis, see: (a) R. Maji, S. C. Mallojjala and S. E. Wheeler, *Chem. Soc. Rev.*, 2018, **47**, 1142–1158; For recent representative examples of computational studies of chiral phosphoric acid catalysis, see: (b) M. N. Grayson and J. M. Goodman, *J. Am. Chem. Soc.*, 2013, **135**, 6142–6148; (c) K. Mori, Y. Ichikawa, M. Kobayashi, Y. Shibata, M. Yamanaka and T. Akiyama, *J. Am. Chem. Soc.*, 2013, **135**, 3964–3970; (d) I. Čorić, J. H. Kim, T. Vlaar, M. Patil, W. Thiel and B. List, *Angew. Chem., Int. Ed.*, 2013, **52**, 3490–3493; (e) K. Kanomata, Y. Toda, Y. Shibata, M. Yamanaka, S. Tuzuki, I. D. Gridnev and M. Terada, *Chem. Sci.*, 2014, **5**, 3515–3523; (f) M. Terada, T. Komuro, Y. Toda and T. Korenaga, *J. Am. Chem. Soc.*, 2014, **136**, 7044–7057; (g) Y. Y. Khomutnyk, A. J. Argüelles, G. A. Winschel, Z. Sun, P. M. Zimmerman and P. Nagorny, *J. Am. Chem. Soc.*, 2016, **138**, 444–456; (h) F. Li, T. Korenaga, T. Nakanishi, J. Kikuchi and M. Terada, *J. Am. Chem. Soc.*, 2018, **140**, 2629–2642; (i) J. Zhang, P. Yu, S.-Y. Li, H. Sun, S.-H. Xiang, J. Wang, K. N. Houk and B. Tan, *Science*, 2018, **361**, 8707–8710; (j) J. Kikuchi, H. Aramaki, H. Okamoto and M. Terada, *Chem. Sci.*, 2019, **10**, 1426–1433; (k) Y. Kwon, J. Li, J. P. Reid, J. M. Crawford, R. Jacob, M. S. Sigman, F. D. Toste and S. J. Miller, *J. Am. Chem. Soc.*, 2019, **141**, 6698–6705; (l) K. Kanomata, Y. Nagasawa, M. Yamanaka, Y. Shibata, F. Egawa, J. Kikuchi and M. Terada, *Chem.–Eur. J.*, 2020, **26**, 3367–3372.
- 21 J. Lapić, A. Višnjevac, M. Cetina, S. Djaković, V. Vrčec and V. Rapić, *J. Mol. Struct.*, 2012, **1019**, 7–15.
- 22 For a review of enantio-convergent substitution reactions using organocatalysts, see: J. Kikuchi and M. Terada, *Chem.–Eur. J.*, DOI: 10.1002/chem.202100439.

